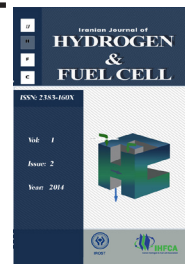


Iranian Journal of Hydrogen & Fuel Cell

IJHFC

Journal homepage://ijhfc.irost.ir



Co₃O₄ spinel protection coating for solid oxide fuel cell interconnect application

Reza Irankhah^{1,*}, Babak Raissi¹, Amir Maghsoudipour¹, Abdullah Irankhah²

¹Department of Ceramic, Materials and Energy Research Center, Tehran, 14155-4777, Iran

²Hydrogen and Fuel Cell Research Lab, Chemical Engineering Department, University of Kashan, Kashan, 87317-51167, Iran

Article Information

Article History:

Received:

25 May 2014

Received in revised form:

7 September 2014

Accepted:

13 September 2014

Keywords

Electrophoretic deposition
Co₃O₄ coating
SOFC interconnect
Oxidation resistance

Abstract

In the present study, electrophoretic deposition (EPD) method in different electric fields (30 – 300 V/cm) was used to apply Co₃O₄ spinel coating to SUS 430 as SOFC interconnect. The coated and uncoated specimens were pre-sintered in air at 800 and 900 °C for 3 h followed by cyclic oxidation at 700 and 800 °C for 500 h, respectively. X-ray diffraction analysis (XRD), Scanning Electron Microscope (SEM) and Energy Dispersive Spectroscopy (EDS) were used for characterization of the prepared samples. The results indicated that the electric field of 100 V was an effective voltage to obtain crack-free coating. A comparison between the oxidation resistance of coated and uncoated specimens indicated that the weight change of the coated specimen was larger than that of the uncoated one during the cyclic oxidation, so the Co₃O₄ coating is not effective for improving the oxidation resistance. According to the obtained results, the oxidation rate constant (K_p) for the coated specimens at 700 and 800°C in air were 2.36×10^{-14} and $3.37 \times 10^{-12} \text{ gr}^2 \text{ cm}^{-4} \text{ s}^{-1}$, respectively.

1. Introduction

Solid oxide fuel cells consist of two electrodes (anode and cathode) separated by the electrolyte. To provide electrical connection between the anode of one cell and the cathode of the neighboring cell, an interconnect component is required. Interconnects should have excellent electrical conductivity and oxidation resistance, good thermal conductivity and thermal expansion coefficient (TEC) matching to those of electrodes and electrolyte [1-3]. The interconnects

for high temperature applications (around 1000°C), are mostly made of ceramic materials such as LaCrO₃. However, due to the fact that ceramic interconnects suffer from some problems such as low electrical conductivity and difficult fabrication procedures [1], metallic interconnects can be used at lower operating temperature (650– 850°C) as an alternative for ceramic ones [4, 5]. Among metallic alloys, Fe–Cr alloys are suitable for being used as interconnect due to their suitable thermal expansion, low cost, excellent formability [6, 7] and good balance between the

*Corresponding author Email address: r.irankhah@gmail.com, r.erankhah@merc.ac.ir

electrical conductivity and the growth rate of Cr_2O_3 [8]. Under SOFC operating temperature, the use of ferritic stainless steel results in Cr migration via Cr_2O_3 scale into the cathode where cathode poisoning is caused [4, 9]. In order to minimize poisoning of the cathode, the interconnect material has to be coated. For this purpose, numerous protective coatings such as Mn/Co [10, 11], LSM/ $\text{Mn}_{1.5}\text{Co}_{1.5}\text{O}_4$ double layer [12], $(\text{Cu}, \text{Mn})_3\text{O}_4$ [13], and Co_3O_4 [8, 14] have been employed. Recent studies have shown that cobalt oxide, cobalt and its composites can be applied by various coating processes on SOFC metallic interconnects. DC magnetron sputtering of Co [15], sol-gel coating of Co [16], pack cementation of Cobalt-base [17] and Physical Vapor Deposition (PVD) of Co thin film [18] on the 430 stainless steel are among these methods. We can also mention the spray-painting or plasma-spraying of Co_3O_4 on crofer 22 [8], slurry coating of Co_3O_4 on Crofer 22 [19], and Co_3O_4 /LSM on Crofer 22, E-Brite and AL 29-4C [20]. In this case, using $\text{Co}(\text{acac}=\text{acetylacetonate})_3$ precursor to synthesize the in-situ Co_3O_4 by Pulsed Injection – Metal Organic Chemical Vapor Deposition (PI-MOCVD) on Fe–22 Cr can also be mentioned [21].

Based on our literature survey, the application of electrophoretic deposition (EPD) method for the preparation of cobalt oxide films has not been considered by researchers. Recently [22], electrophoretic deposition (EPD) of nano-cobalt oxide (Co_3O_4) particle was investigated to develop coatings with potential applications in many fields. The EPD technique has recently attracted much attention for producing thin and thick ceramic layers. In this process, ceramic particles dispersed in a liquid medium under a DC electric field migrate towards an opposite electrode and consequently deposit there [23]. Electrophoretic deposition (EPD) has advantages such as short formation time, easy control over the thickness and morphology of the deposited film as well as no needs for complicated equipment [24]. In this work, EPD was used to insert the Co_3O_4 spinel coating on SUS 430 as a SOFC interconnect. Different EPD electric fields were examined to determine the optimum conditions for obtaining layers of desired

quality. At the next step, long term cyclic oxidation resistance was investigated.

2. Experimental

2.1. Preparation of SUS 430

SUS 430 was used as the interconnect substrate and prepared in pieces (as an electrode in EPD process) with a dimension of $20 \times 20 \times 3$ (mm \times mm \times mm). Prior to deposition, the substrates were grounded with SiC abrasive papers of # 400, 800 and 1200 and then cleaned in acetone in an ultrasonic bath for 20 min.

2.2. Suspension preparation and EPD

The Co_3O_4 powder (1.02543, Merck) with an average particle size of $5 \mu\text{m}$ was used as the starting material in EPD process. In order to prepare a stable and agglomerate-free suspension of Co_3O_4 particles, the 1 g/L suspension of Co_3O_4 (0.025 gr) in the acetone was first sonicated for 20 min. The deposition experiments of Co_3O_4 particles were performed using a homemade EPD setup (Fig. 1). Also, Conductivity measurements of the prepared suspensions were carried out using

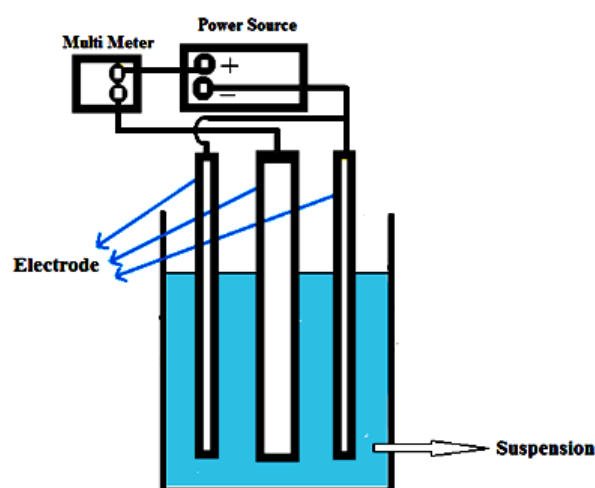


Fig. 1. The schematic of EPD setup.

a WTW - Inolab (Weilheim, Germany) conductivity meter. In order to prepare stable suspensions during deposition, the poly ethylene imine (PEI) dispersing

agent was employed. After adding the dispersant (before deposition), the suspension was sonicated for 20 min again to ensure adequate dispersion of the PEI across the medium. The zeta potential measurement was performed for each suspension with and without the dispersing agent using a Malvern.3000 HAS Zeta-sizer. A DC high voltage power supply was used for the deposition of Co_3O_4 on SUS 430 electrodes at a distance of 1 cm. The deposition duration and potential was determined to be 30–300 V/cm and 1 min, respectively. The XRD analysis, performed (UNISANTIS, XMD300, Germany) using a Cu $K\alpha$ mono chromatized radiation source as well as energy dispersive analysis (EDS) and scanning electron microscope (SEM, Stereo Scan S360, Oxford) were employed to characterize the deposited layers.

2.3. Pre-sintering and cyclic Oxidation

The as-deposited coatings (in 100 V) were pre-sintered in air at 800 °C and 900 °C for 3 h followed by oxidizing at 700 °C and 800 °C for 500 h, respectively. To test the cyclic oxidation behavior, the specimens were cooled to room temperature every 50 h and weighted using an electronic balance (10^{-5} gr accuracy).

3. Result and discussion

3.1. The effect of dispersant on EPD current and conductivity

Since the Co_3O_4 /acetone suspension was not adequately stable, poly ethylene imine (PEI) was employed as dispersing agent to enhance the stability of the particles across the medium. After the addition of PEI, the prepared suspension was sonicated for 20 min again to achieve a homogeneous suspension suitable for the EPD process. It was observed that the addition of one drop of PEI increased the electrical conductivity of the suspension from 0.2 $\mu\text{S}/\text{cm}$ to 2.6 $\mu\text{S}/\text{cm}$. Moreover, it increased the zeta potential value from -10 mV to +38 mV which means that the surface charge of particles has changed in the presence of PEI.

PEI is a cationic polyelectrolyte with unit formula of $-\text{[CH}_2\text{-CH}_2\text{-NH]n-}$. It was used, as a dispersant, to modify the surface charge of the Co_3O_4 powders. The adsorption of the PEI on the particle surfaces resulted in a good dispersion of the suspension with a positive charge. Similar tendencies have been observed in other suspensions of ceramic oxides [18, 25, and 26]. The protonation of the amine $-\text{NH}$ groups in PEI molecules and subsequent expansion of the poly ions due to mutual charge repulsion are assignable to the modification of the Co_3O_4 surface charge.

As it was mentioned above, different electric fields were applied for EPD process. Fig. 2 shows the weight of deposited Co_3O_4 on SUS 430 substrate from an acetone based suspension containing PEI at 30–300 V. The deposition weight is increased as a function of applied electric field because of higher deposition rate of particles. The results are in accordance with the Hamaker Eq [24].

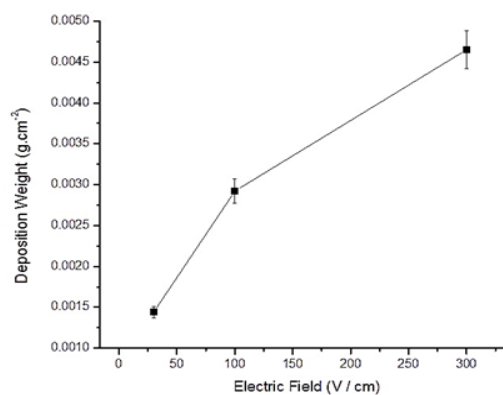


Fig. 2. Deposition weight as a function of electric field for 1 min deposition duration.

Current density during EPD versus time of deposition for Co_3O_4 suspension with PEI dispersant indicated that the current decreased with time during EPD for all experiments. Because of the formation of an insulating layer on the electrode, the electric field influencing electrophoresis as well as the current density during EPD has been decreased [24]. In contrast, higher voltages gave rise to higher driving forces for particles movement and consequently higher current densities (Fig.3).

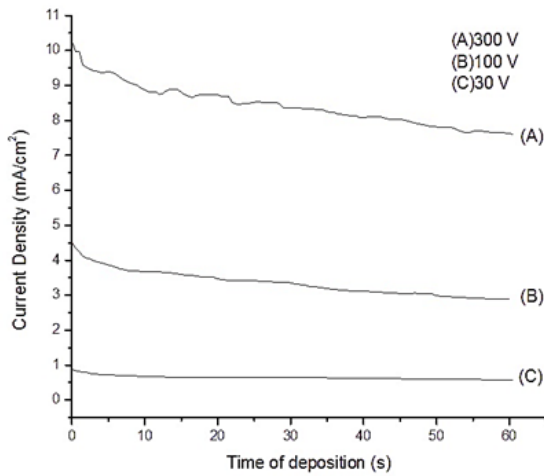


Fig. 3. Current density in EPD of Co_3O_4 suspension with PEI at different voltage.

The Co_3O_4 layers formed at 30-300 V with and without PEI were shown in Fig. 4. As it shown, the deposition yield increased with the addition of PEI where a good adherence to the substrate was obtained (Fig. 4b and 4c). However, in depositions carried out without PEI (Fig. 4a and 4b), the coating was prone to poor adhesion. It is obvious that the thickness of the spinel layer was enhanced through the addition of PEI to the suspension. It has to be noted that for oxidation tests, 2-side coated specimens were used (Fig. 4, e).

3.2. Effect of electric field strength on surface morphology

To study the effect of the electric field strength on the quality of the deposited layer, EPD was performed in different potentials of 100 and 300 V. Fig. 5 (a - c) depicts the SEM images of as-deposited Co_3O_4 spinel coatings at 100 and 300 V, respectively. It can be observed from Fig. 5 that as the electric field strength is increased, a more porous microstructure has formed which is in agreement with the result of other researchers [24, 27]. Besides, the deposited layer in 300 V resulted in the formation of micro cracks that could be attributed to the evaporation of acetone trapped within the layer during deposition (Fig 5. (c) [28].

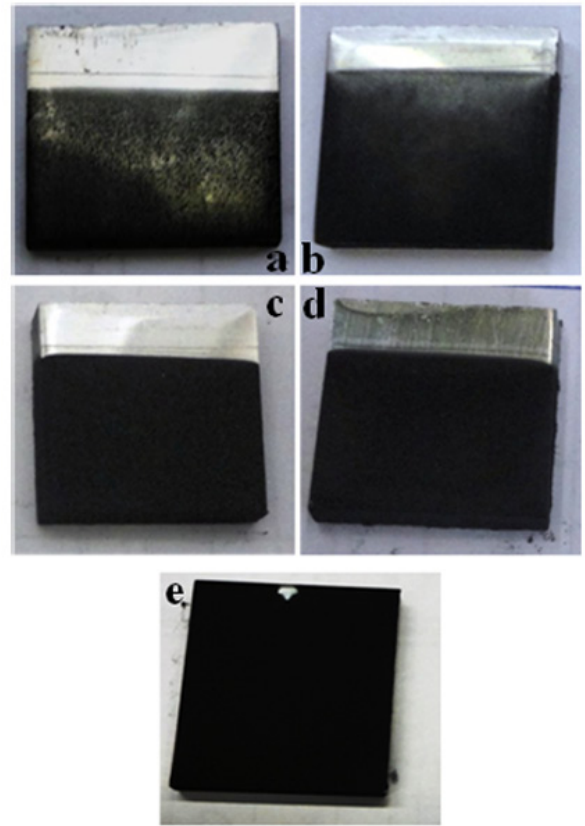


Fig. 4. As deposited layer of Co_3O_4 on SUS 430 at a) 30 V without PEI , b) 100 V without PEI, c) 100 V with PEI, d) 300 V with PEI - 1side was coated and e) 100 V with PEI – 2 side was coated.

3.3. Effect of pre-sintering atmosphere on oxidation resistance

3.3.1. Cyclic oxidation in 700 °C

The squared weight change per area versus oxidation duration (10 cycles) for coated and uncoated specimen is shown in Fig .6. The curves after 50 h are linear and obey the Wagner theory based on the following relation (equation 1):

$$(\Delta W/A)^2 = K_p t \quad (1)$$

Where, ΔW is mass gain, A is the surface of coated samples, t is time of oxidation and K_p is the oxidation parabolic rate constant [29]. It is obvious that the weight change of the coated specimen was larger than

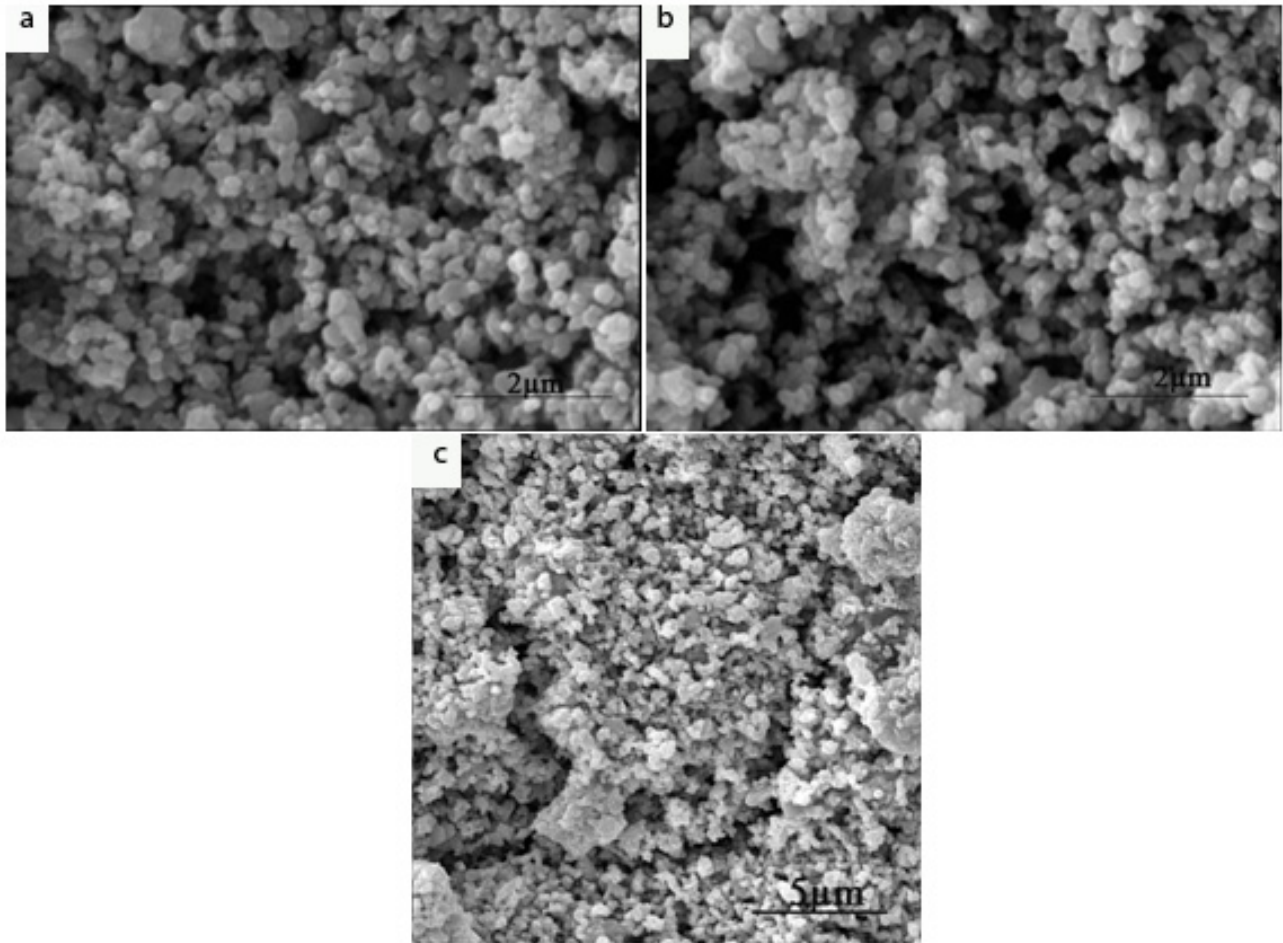


Fig. 5. The SEM micrograph of as-deposited Co_3O_4 film in (a) 100 V, (b) 300 V, (c) 300 V cracked layer (deposition time for all voltage was 1 min).

that of the uncoated one during the cyclic oxidation. Oxidation rate constant for coated and uncoated specimens are 2.36×10^{-14} and $3.40 \times 10^{-14} \text{ gr}^2 \cdot \text{cm}^{-4} \cdot \text{s}^{-1}$, respectively. Although the weight change for Co_3O_4 coated specimen during oxidation is more than that of the uncoated sample, oxidation rate constant for the uncoated specimen is nearly 1.45 times more than that of the coated one.

3.3.2. Cyclic oxidation in 800 °C

To study the effect of oxidation temperature on oxidation rate constant, the uncoated SUS 430 and coated specimens were pre-sintered in air at 900 °C for 3 h followed by 10 cycles, each including 50 h at 800 °C in accordance with the operational temperature of SOFC cathode.

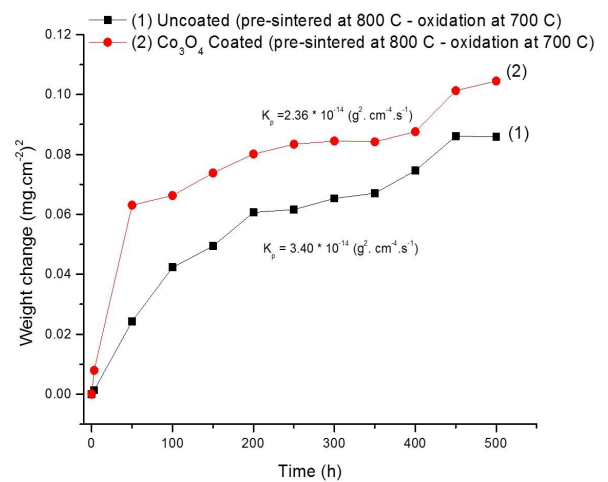


Fig. 6. Cyclic oxidation test and weight changes of the uncoated and coated substrates vs. Oxidation time at 700 °C.

Fig. 7 shows the weight changes of the uncoated and coated substrates as a function of oxidation time during cyclic oxidation test. As shown by this figure, the K_p value for coated pre-sintered specimens in air is $3.37 \times 10^{-12} \text{ gr}^2 \cdot \text{cm}^{-4} \cdot \text{s}^{-1}$. The K_p for the uncoated specimen was calculated to be $1.96 \times 10^{-12} \text{ gr}^2 \cdot \text{cm}^{-4} \cdot \text{s}^{-1}$. Hence, sintering in air was observed to increase it by nearly 1.7-folds in comparison with the uncoated specimen. Laring and Norby suggested that Co_3O_4 coating does not have a beneficial effect on the oxidation behavior of a chromia forming steel [30]. Therefore Annette et al investigated the oxidation behavior of uncoated and Co_3O_4 coated Fe-22Cr and reported that this coating decreased the oxidation rate compared with the uncoated alloy [8]. In the present study, results indicated that the pre-sintered Co_3O_4 coating in air is not suitable for improving the oxidation resistance (see Fig. 6 (1 and 2), Fig. 7 (A and B)).

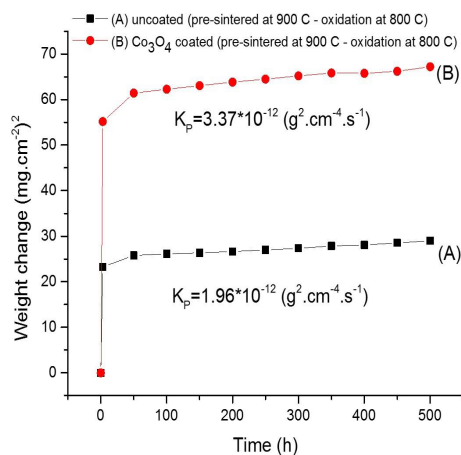


Fig. 7. Cyclic oxidation test and weight changes of the uncoated and coated substrates vs. Oxidation time at 800 °C.

The SEM cross sectional observations used for the purpose of imaging and chemical microanalysis of the layers. Fig. 8 shows the cross-sectional image and EDS elements line scan of the substrate and oxide scale developed on uncoated specimen, after 500 h of oxidation in air at 800°C. The oxide scale layer with a thickness about 43 μm was continuous, uniform and it consisted mainly of Cr, Fe, O with a small amount of Mn. The remaining Au from sample preparation

procedure was also detected by SEM. It is conspicuous in Fig. 8 (c and d) that the chromium was enriched in the oxide layer, with the amount of Cr in the inner oxide higher than in the outer oxide.

Fig. 9 presents the cross-sectional SEM image and EDS line scans along the cross section of Co_3O_4 coated specimen after 500 h of oxidation in air at 800°C. It is obvious that three layers can be distinguished for the coated sample (Fig. 9a): coating layer, oxide layer and substrate. A good adhesion, without cracking or discontinuity, between the coating and the substrate is observed. The inward diffusion of oxygen anions facilitates the formation of a more compact and adherent oxide layer [53]. A dense, adherent thermally grown spinel (oxide layer) acted as an effective barrier against outward diffusion of Cr and Fe cations, which decreased the formation of voids and micro-cracks at oxide/substrate interface and increased the spallation resistance [13, 17].

It may result in low contact resistance or good electrical connection between the anode of one cell and the cathode of the neighboring cell [31-34]. According to the elemental EDS analysis of oxide and coating layer, the coating consists mainly of Co, Fe, Cr and O. The Chromium is present in the steel and increases in region B and decreases severely along the oxidized coating layer (C Area), thus, it can be concluded that the Co_3O_4 coating prevented the diffusion of Cr cations into the surface, which in other words means no Cr would poison the SOFC cathode [4, 9, 35-39]. Chromium contamination of SOFC cathodes has been observed by several groups of researchers [40-51].

3.3.3. Characterization of oxidation products by XRD analysis

Oxidation studies by XRD analysis (Fig. 10) identify the oxide scales formed during cyclic oxidation on the uncoated and Co_3O_4 spinel coated specimen. The XRD pattern analysis (Fig. 10- (A)) of the uncoated SUS 430 oxidized at 800°C in air for 500 h revealed that the specimen was composed of Cr and Fe oxide phases. In contrast, the coated specimen (Fig. 10 - (B)) showed characteristic CoFe_2O_4 , CoCrO_4 , Fe_2O_3 phases. Since

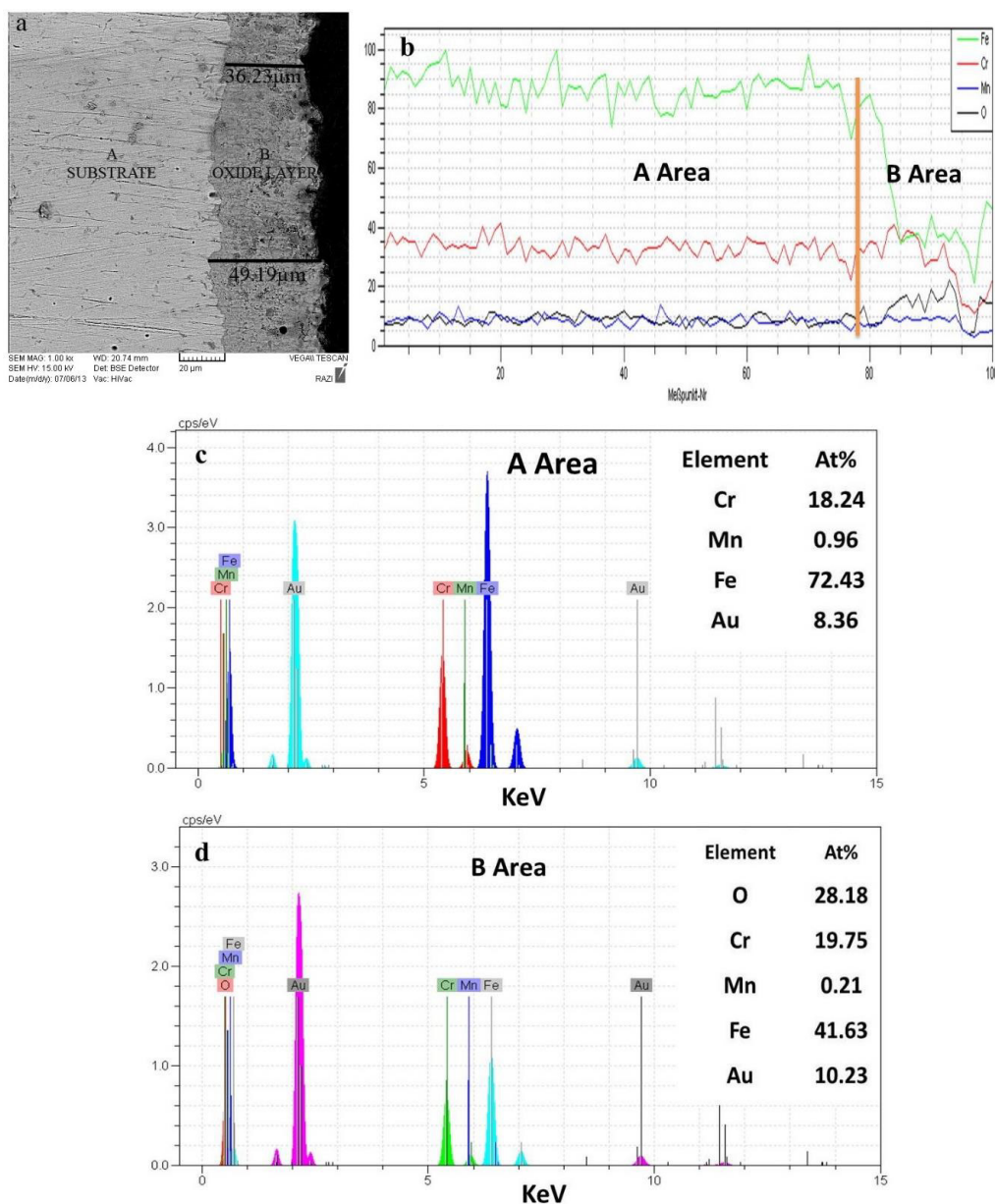


Fig. 8. SEM cross section (a), (b) EDS line scan, (c) A area EDS analysis and B area EDS analysis (d) of uncoated sample after oxidation at 800°C for 500 h.

the penetration depth of XRD is higher than the film thickness, the Fe-Cr phase was also detected. Inward oxygen diffusion and outward chromium, iron cations diffusion toward the oxide surface /coating resulted in the formation of Co/Cr and Co/Fe oxide phases [8, 52, and 53].

4. Conclusion

The EPD technique was used to apply Co_3O_4 layer on SUS 430 ferritic stainless steel. Results of this study demonstrate that EPD is a feasible method of fabricating Co_3O_4 coating. Pre-sintering of the Co_3O_4 coating in air was also investigated. The oxidation tests of pre-sintered specimens in air at 700 and 800°C indicated that the weight change of coated specimens

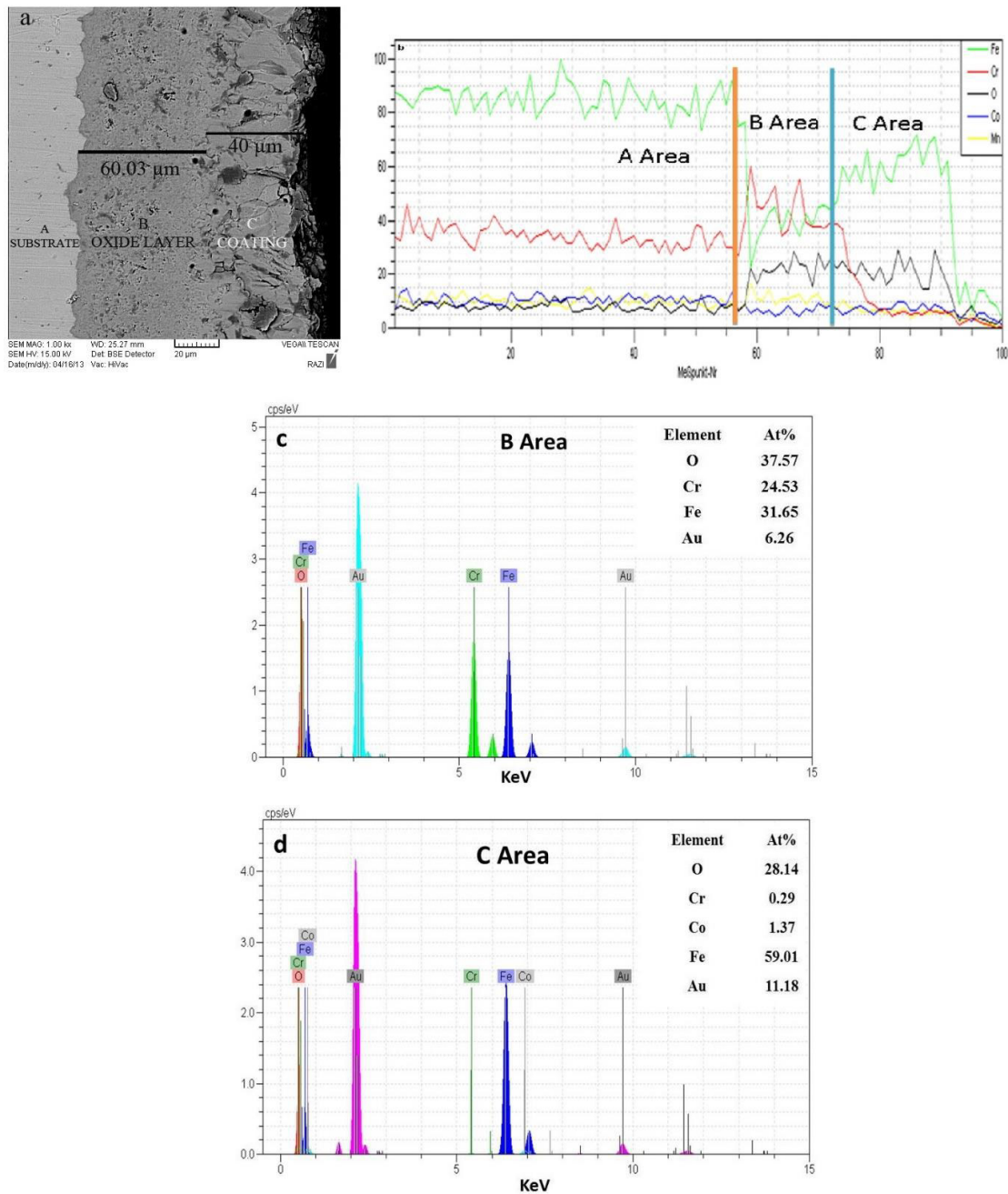


Fig. 9. SEM cross section (a), (b) EDS line scan, (c) B area EDS analysis and C area EDS analysis (d) of Co_3O_4 coated sample after oxidation at 800°C for 500h.

was larger than that of uncoated ones. It appears that the pre-sintered Co_3O_4 coating in air is not effective for improving the oxidation resistance of interconnect.

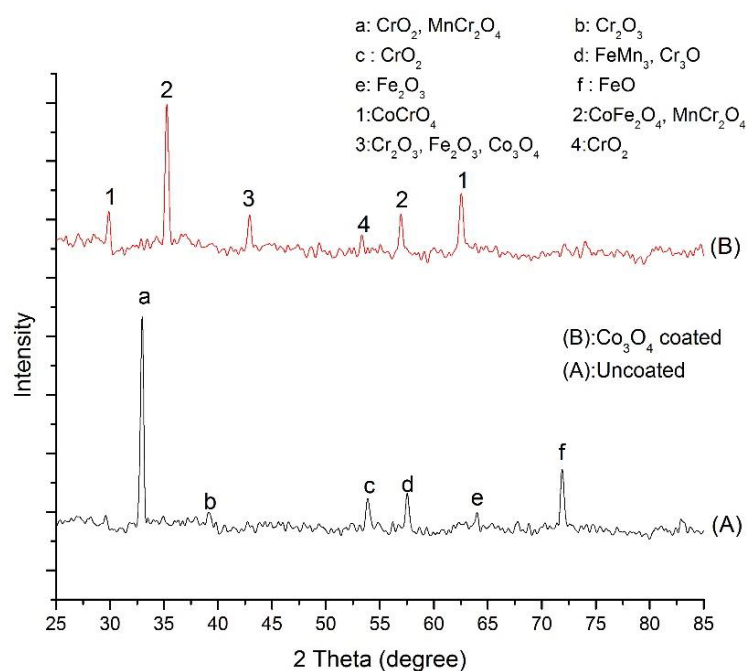


Fig. 10. The XRD patterns of cyclic oxidized specimens at 800 °C in air for 500 h (A) uncoated SUS430 (B) Co₃O₄ coated.

5. References

- Fontana S, Amendola R, Chevalier S, Piccardo P, Caboche G, Viviani M, Molins R, Sennour M, Metallic interconnects for SOFC: Characterization of corrosion resistance and conductivity evaluation at operating temperature of differently coated alloys, *Journal of PowerSources*. 2007;171(2): 652-62.
- Zhu WZ, Deevi SC, Opportunity of metallic interconnects for solid oxide fuel cells: a status on contact resistance, *Materials Research Bulletin*. 2003;38(6): 957-72.
- Zhu WZ, Deevi SC, Development of interconnect materials for solid oxide fuel cells, *Materials Science and Engineering: A*. 2003; 348(1-2): 227-43.
- Shaigan N, Qu W, Ivey DG, Chen W, A review of recent progress in coatings, surface modifications and alloy developments for solid oxide fuel cell ferritic stainless steel interconnects, *Journal of Power Sources*. 2010; 195(6): 1529-42.
- Ebrahimifar H, Zandrahimi M. Mn coating on AISI 430 ferritic stainless steel by pack cementation method for SOFC interconnect applications, *Solid State Ionics*. 2011; 183(1): 71-9.
- Z. Yang, K.S. Weil, D.M. Paxton, J.W. Stevenson, Selection and Evaluation of Heat-Resistant Alloys for SOFC Interconnect Applications, *J. Electrochem. Soc*. 2003; 150: 1188
- Batani MR, Wei P, Deng X, Petric A, Spinel coatings for UNS 430 stainless steel interconnects, *Surface and Coatings Technology*. 2007; 201(8): 4677-84.
- Hansson AN, Linderroth S, Mogensen M, Somers MAJ, Inter-diffusion between Co₃O₄ coatings and the oxide scale on Fe-22Cr, *Journal of Alloys and Compounds*. 2007; 433(1-2): 193-201.
- Fergus JW. Metallic interconnects for solid oxide fuel cells, *Materials Science and Engineering: A*. 2005; 397(1-

- 2): 271-83.
10. Wu J, Gemmen RS, Manivannan A, Liu X, Investigation of Mn/Co coated T441 alloy as SOFC interconnect by on-cell tests, *International Journal of Hydrogen Energy*. 2011: 36(7): 4525-9.
11. Hoyt KO, Gannon PE, White P, Tortop R, Ellingwood BJ, Khoshuei H, Oxidation behavior of $(\text{Co},\text{Mn})_3\text{O}_4$ coatings on pre oxidized stainless steel for solid oxide fuel cell interconnects, *International Journal of Hydrogen Energy*. 2012: 37(1): 518-29.
12. Yoo J, Woo S-K, Yu JH, Lee S, Park GW, $\text{La}_{0.8}\text{Sr}_{0.2}\text{MnO}_3$ and $(\text{Mn}_{1.5}\text{Co}_{1.5})\text{O}_4$ double layer coated by electrophoretic deposition on Crofer 22 APU for SOEC interconnect applications, *International Journal of Hydrogen Energy*. 2009:34(3): 1542-7.
13. Petric, A. and Ling, H, Electrical Conductivity and Thermal Expansion of Spinel at Elevated Temperatures, *Journal of the American Ceramic Society*. 2007: 90: 1515–1520.
14. Deng X, Wei P, Bateni MR, Petric A, Cobalt plating of high temperature stainless steel interconnects, *Journal of Power Sources*. 2006:160(2): 1225-9.
15. Macauley C, Gannon P, Deibert M, White P, The influence of pre-treatment on the oxidation behavior of Co coated SOFC interconnects, *International Journal of Hydrogen Energy*. 2011:36(7): 4540-8.
16. Dayaghi AM, Askari M, Gannon P, Pre-treatment and oxidation behavior of sol–gel Co coating on 430 steel in 750°C air with thermal cycling, *Surface and Coatings Technology*. 2012: 206(16): 3495-500.
17. Ebrahimi far H, Zand rahimi M, Oxidation and electrical behavior of AISI 430 coated with cobalt spinels for SOFC interconnect applications, *Surface and Coatings Technology*. 2011: 206(1): 75-81.
18. Lacey R, Pramanick A, Lee JC, Jung J-I, Jiang B, Edwards DD, Naum Robert, Misture T. Scott, Evaluation of Co and perovskite Cr-blocking thin films on SOFC interconnects, *Solid State Ionics*. 2010: 181(27–28): 1294-302.
19. Persson ÅH, Mikkelsen L, Hendriksen PV, Somers MAJ, Interaction mechanisms between slurry coatings and solid oxide fuel cell interconnect alloys during high temperature oxidation, *Journal of Alloys and Compounds*. 2012: 521(0): 16-29.
20. Palcut M, Mikkelsen L, Neufeld K, Chen M, Knibbe R, Hendriksen PV, Efficient dual layer interconnect coating for high temperature electrochemical devices, *International Journal of Hydrogen Energy*. 2012: 37(19): 14501-10.
21. Burriel M, Garcia G, Santiso J, Hansson AN, Linderroth S, Figueras A, Co_3O_4 protective coatings prepared by Pulsed Injection Metal Organic Chemical Vapour Deposition, *Thin Solid Films*. 2005: 473(1): 98-103.
22. Daixiong Zhang, Xueming Li, Xiaogang Guo, Chuan Lai, Fabrication of cobalt oxide (Co_3O_4) coating by electrophoretic deposition, *Materials Letters* 126 (2014) 211–213.
23. Kaya C, Kaya F, Su B, Thomas B, Boccaccini AR, Structural and functional thick ceramic coatings by electrophoretic deposition, *Surface and Coatings Technology*. 2005: 191(2–3): 303-10.
24. Besra L, Liu M, A review on fundamentals and applications of electrophoretic deposition (EPD), *Progress in Materials Science*. 2007: 52(1): 1-61.
25. Fengqiu Tang, T.U, Kiyoshi ozawa, yoshio sakka. Effect of polyethylenimine on the dispersion and electrophoretic deposition of nano-sized titania aqueous suspensions. *European ceramic society*, 26, 2006, pages 1555-1560.
26. Kai Cai, M. O, Hideyuki Murayama, Influence of polyelectrolyte dispersants on the surface chemical properties of aluminum in aqueous suspension. *Colloids and surfaces A: physicochemical. Eng. Aspects*, 284-285,

- 2006, 458-463.
27. Zhang H, Zhan Z, Liu X, Electrophoretic deposition of $(\text{Mn,Co})_3\text{O}_4$ spinel coating for solid oxide fuel cell interconnects, *Journal of Power Sources*. 2011: 196(19): 8041-7.
28. Chen C-C, Jwo C-S, Teng T-P, De composition of formaldehyde by EPD photo catalyst filters in HVAC, *Particuology*. 2011: 9(5): 497-501.
29. C. Wagner, *Z. Phys. Chem.* 1933: B21: 42.
30. Y. Larring, T. Norby, Spinel and Perovskite Functional Layers Between Plansee Metallic Interconnect (Cr 5 wt % Fe 1 wt% Y_2O_3) and Ceramic $(\text{La}_{0.85}\text{Sr}_{0.15})_{0.91}\text{MnO}_3$ Cathode Materials for Solid Oxide Fuel Cells, *J. Electro chem. Soc.* 2003: 147: 251–3256.
31. Liu Y, Chen DY, Protective coatings for Cr_2O_3 -forming interconnects of solid oxide fuel cells, *International Journal of Hydrogen Energy*. 2009: 34 (22): 9220-6.
32. Geng S, Qi S, Zhao Q, Zhu S, Wang F, Electroplated Ni– Fe_2O_3 composite coating for solid oxide fuel cell interconnect application, *International Journal of Hydrogen Energy*. 2012: 37 (14) 10850-6.
33. Geng S, Wang Q, Wang W, Zhu S, Wang F, Sputtered Ni coating on ferritic stainless steel for solid oxide fuel cell interconnect application, *International Journal of Hydrogen Energy*. 2012: 37 (1): 916-20.
34. Shujiang Geng, Yandong Li, Zhonghe Ma, Linlin Wang, Linna Li, Fuhui Wang, Evaluation of electrodeposited Fe–Ni alloy on ferritic stainless steel solid oxide fuel cell interconnect, *Journal of Power Sources*. 2010: 195 (10): 3256-3260.
35. Yanjie Xu, Zhaoyin Wen, Shaorong Wang, Tinglian Wen, Cu doped Mn–Co spinel protective coating on ferritic stainless steels for SOFC interconnect applications, *Solid State Ionics*. 2011: 192(1): 561-564.
36. Shaigan N, Qu W, Ivey Dg, Chen W, A review of recent progress in coatings, surface modifications and alloy developments for solid oxide fuel cell ferritic stainless steel interconnects, *Journal of Power Sources*. 2010: 195(6): 1529-42.
37. Fergus JW, Metallic interconnects for solid oxide fuel cells, *Materials Science and Engineering: A*. 2005: 397(1–2): 271-83.
38. Geng S, Zhu J, Brady MP, Anderson HU, Zhou X-D, Yang Z, A low - Cr metallic interconnect for intermediate-temperature solid oxide fuel cells, *Journal of Power Sources*. 2007: 172 (2): 775-81.
39. Yang Z, Xia G, Singh P, Stevenson JW, Electrical contacts between cathodes and metallic interconnects in solid oxide fuel cells, *Journal of Power Sources*. 2006: 155 (2): 246-52.
40. Zhenguo Yang, Guan-Guang Xia, Xiao-Hong Li, Jeffry W. Stevenson, $(\text{Mn,Co})_3\text{O}_4$ spinel coatings on ferritic stainless steels for SOFC interconnect applications, *International Journal of Hydrogen Energy*. 2007: 32(16): 3648-3654.
41. Michael Krumpelt, Thomas Kaun, Terry A. Cruse, Mark C. Hash, SOFC Research and Development, Office of Fossil Energy Fuel Cell Program, Annual Report FY: 2004.
42. Dayaghi, A. M, Masoud Askari, Paul Gannon, Pre-treatment and oxidation behavior of sol–gel Co coating on 430 steel in 750 °C air with thermal cycling, *Surface and Coatings Technology*. 2012: 206(16): 3495-3500.
43. Kurokawa, H, Craig P. Jacobson, Lutgard C. DeJonghe, Steven J. Visco, Chromium vaporization of bare and of coated iron–chromium alloys at 1073 K, *Solid State Ionics*. 2007: 178 (3–4): 287-296.
44. Fergus, J. W, Synergism in the design of interconnect alloy–coating combinations solid for oxide fuel cells, *Scripta Material A*. 2011: 65 (2): 73-77.

45. Wu, J, Christopher D. Johnson, Randall S. Gemmen, Xingbo Liu, The performance of solid oxide fuel cells with Mn–Co electroplated interconnects as cathode current collector, *Journal of Power Sources*. 2009: 189 (2): 1106-1113.
46. Shaigan, N, Douglas G. Ivey, Weixing Chen, Co/ LaCrO₃ composite coatings for AISI 430 stainless steel solid oxide fuel cell interconnects, *Journal of Power Sources*. 2008: 185 (1): 331-337.
47. Deng, X, Ping Wei, M. Reza Bateni, Anthony Petric, Cobalt plating of high temperature stainless steel interconnects, *Journal of Power Sources*. 2006: 160 (2): 1225-1229.
48. Froitzheim. J, S. Canovic, M. Nikumaa, R. Sachitanand, L.G. Johansson, J.E. Svensson, Long term study of Cr evaporation and high temperature corrosion behaviour of Co coated ferritic steel for solid oxide fuel cell interconnects, *Journal of Power Sources*. 2012: 220 (0): 217-227.
49. Palcut, M, Lars Mikkelsen, Kai Neufeld, Ming Chen, Ruth Knibbe, Peter Vang Hendriksen, Efficient dual layer interconnect coating for high temperature electrochemical devices, *International Journal of Hydrogen Energy*. 2012: 37 (19): 14501-14510.
50. Wu J, Randall S. Gemmen, Ayyakkannu Manivannan, Investigation of Mn/Co coated T441 alloy as SOFC interconnect by on-cell tests, *International Journal of Hydrogen Energy*. 2011: 36 (7): 4525-4529.
51. Persson, Å. H, L. Mikkelsen, P.V. Hendriksen, M.A.J. Somers, Interaction mechanisms between slurry coatings and solid oxide fuel cell interconnect alloys during high temperature oxidation, *Journal of Alloys and Compounds*, 2012: 521 (0): 16-29.
52. Liu Y, Chen DY, Protective coatings for Cr₂O₃-forming interconnects of solid oxide fuel cells, *International Journal of Hydrogen Energy*. 2009: 34 (22): 9220-6.
53. Qu, W, Li Jian, Douglas G. Ivey, Josephine M. Hill, Yttrium, cobalt and yttrium/cobalt oxide coatings on ferritic stainless steels for SOFC interconnects, *Journal of Power Sources*. 2006: 157 (1): 335-350.